

Supporting Information

Reduction of CO₂ to CO by an Iron Porphyrin catalyst in the presence of Oxygen

Biswajit Mondal[#], Pritha Sen[#], Atanu Rana, Dibyajyoti Saha, Purusottom Das, Abhishek Dey*

School of Chemical Sciences, Indian Association for the Cultivation of Science, 2A & 2B
Raja S.C. Mullick Road, Kolkata, 700032, WB, India

icad@iacs.res.in

[#]These authors have contributed equally.

Table of Contents

Sl.No.	Content	Page No.
1.	Experimental Details	S2
2.	DFT calculations	S3
3.	CV data with increasing concentration of CO ₂ -Figure S1	S4
4.	Aerobic CV of FeFc ₄ and in the presence of CO ₂ -Figure S2	S4
5.	Aerobic CV of FeFc ₄ and background data -Figure S3	S5
6.	CV data of FeFc ₄ with increasing concentration of O ₂ -Figure S4	S5
7.	Bulk electrolysis data @-2.2V-Figure S5	S6
8.	CV data of catalyst after and before bulk electrolysis- Figure S6	S6
9.	Data for FePf porphyrins -Fig. S7	S7
10.	DFT optimised structures of Fe(II)-O ₂ and Fe(II)-CO ₂ ²⁻ adduct -Figure S8	S7
11.	Estimate of % PROS for various iron porphyrins of interest- Table S1	S8

12.	Estimate of % Faradaic yield for FeFc ₄ during CO ₂ reduction and ORR- Table S2	S9
13.	Data for FePf porphyrins -Figure S9	S9
14.	ORR using Pt vs GC electrode as counter-Figure S10	S10
15.	Background data and CV before and after bulk electrolysis- Figure S11	S10
16.	Data for Fe(tBu) ₄ - Figure S12	S11
17.	Coordinates of optimized geometry -Table S3	S12-S14
18.	References	S15

Experimental Details

Materials. All reagents were of the highest grade commercially available and were used without further purification.

Instrumentation. UV–vis absorption data were taken in an Agilent technologies spectrophotometer model 8453 fitted with a diode-array detector. All electrochemical experiments were performed using a CH Instruments (modelCHI710D Electrochemical Analyser).

Synthesis. α_4 -Tetra-2-(4-ferrocenyl-1,2,3-triazolyl)-phenylporphyrinato Iron (FeFc₄) catalyst has been prepared in our laboratory and has been synthesized as reported.¹ The FePf is synthesized as reported in literature.²

Cyclic Voltammetry Experiment. Homogeneous CV experiments were done in acetonitrile solution containing mostly 100mM tetrabutylammonium perchlorate (TBAP) (supporting electrolyte) using Glassy Carbon as working electrode, Pt wire as the counter electrode and AgCl/Ag as the reference electrode. The scan rate is maintained at 100mV/s unless otherwise indicated. Ferrocene groups in FeFc₄ acts as internal standard and the x-axis is adjusted to Fc⁺⁰ based on this. In some experiments edge plane pyrolytic graphite (EPG) is used as working electrode.

A 0.5 mM solution of catalyst in 10 mL of 0.1 M TBAP/MeCN in 3M PhOH electrolyte was prepared for conducting controlled potential electrolysis experiments. We have used glassy carbon as standard reference electrode, Pt electrode as counter and Ag/AgCl electrode as reference. 5 mL of 0.1 M TBAP/MeCN electrolyte with 20 mM tetrabutylammonium acetate was filled to the counter electrode chamber.³ Kolbe reaction was used to generate CO₂ and ethane from the oxidation of this soluble acetate, thereby preventing formation of solvent/PhOH oxidation by-products. Both compartments were sealed to be gas-tight. Using acrylic body gas flow meter purchased from Chemix speciality Gases and Equipment, the concentration of CO₂ in the solution was varied by changing the CO₂ to O₂ partial pressure. Two different digital gas flow meters with flow tubes (One for CO₂ gas control and another for oxygen gas control) was used in this experiment. A homogeneous mixture of the two gases was made previously before passing them to the electrochemical cell. During the CO₂-O₂ concentration dependence experiments, different CO₂/O₂ gas partial pressures were used varying the partial pressure of CO₂ to 100, 75, 50 and 25%. During the experiments each time the gas mixture was purged for one hour into the solution containing the electrolyte and catalysts and then the data was recorded. Formate was determined by ionic chromatography (02919, Eco IC, Metrohm)

UV-Vis Experiment.

Iron porphyrins are reduced to Fe(0) porphyrin with 3 equivalent of Na-Hg.⁴ Na-anthracenide is also used as reducing agent for some cases.⁵ THF is used as solvent and slight amount of MeOH is used to activate Na-Hg. Saturated solution of O₂, CO₂ and Ar in phenol in THF are prepared. UV-Vis kinetics are measured by adding specified amount of these solution into 20 μM Fe(0) porphyrin solution under stirring condition at ambient temperature. Fe(0) porphyrin has a characteristic band at ~ 440 nm and the decay this band is monitored with respect to time to get the kinetics.

H₂O₂ Detection. A xylenol orange assay was used to detect H₂O₂ produced during O₂ reduction under homogeneous conditions. A 4.9 mg portion of Mohr's salt and 3.9 mg of xylenol orange were dissolved in 5 mL of 250 mM H₂SO₄ and stirred for 10 min. A 200 μL portion of this solution was taken in 1.8 mL of triple distilled water, and a calibration curve for quantitative estimation of H₂O₂ was obtained by adding 20 μL aliquots of H₂O₂ having different concentrations and recording their absorbance at 560 nm. The concentrations of H₂O₂ used were 0.05 μM, 0.1 μM, 0.5 μM, 1 μM, 2.5 μM, 5 μM, 10 μM, and 100 μM. A 200 μL portion

of the xylenol orange H_2SO_4 mixture was added to 1.8 mL of H_2O in a cuvette, and the absorbance was recorded. A 100 μL portion of test sample from bulk electrolysis cell containing 1 mM FeFc_4 was extracted with 200–400 μL of H_2O and CHCl_3 mixed solvent. 20 μL of this aqueous extract was added to the cuvette containing the xylenol orange and H_2SO_4 mixture. Absorbance for this was recorded. The absorbance of the above solution (after subtracting the control) at 560 nm is fitted in the calibration curve (obtained as described above) to get the corresponding H_2O_2 concentrations. This concentration is scaled accounting for dilution to get the concentration of H_2O_2 produced in the original $\alpha_4\text{-FeFc}_4$ solution. The % Faradaic yield is calculated from the amount of charged consumed in the bulk electrolysis experiments as discussed above.

DFT Calculations. The Density Functional Theory⁶ calculations of the complexes were carried out using BP86 functional in unrestricted formalism. For these complexes a split basis set (6-311g* on Fe and 6-31g* on C, H, O and N atoms) were used. The single point energy correction of the optimized structures was carried out using 6-311+g* basis set on all atoms. The frequencies were calculated on the optimized structures.

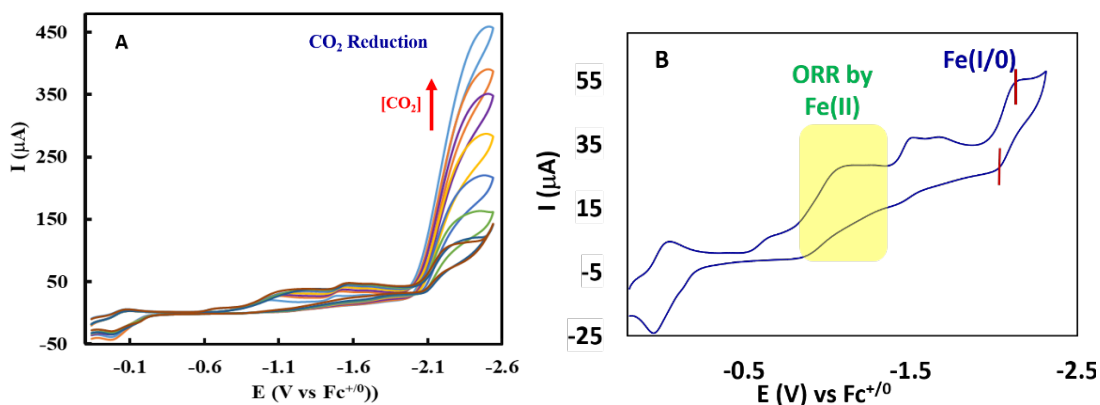


Figure S1. (A) The CV of FeFc_4 with increasing CO_2 concentration (with PhOH) (B) in the presence of oxygen (without PhOH) in 3M phenol in acetonitrile with glassy carbon as working electrode, Pt counter and AgCl/Ag as reference electrode. 100 mM tetrabutylammonium perchlorate is used as supporting electrolyte. Scan rate = 100 mV/s.

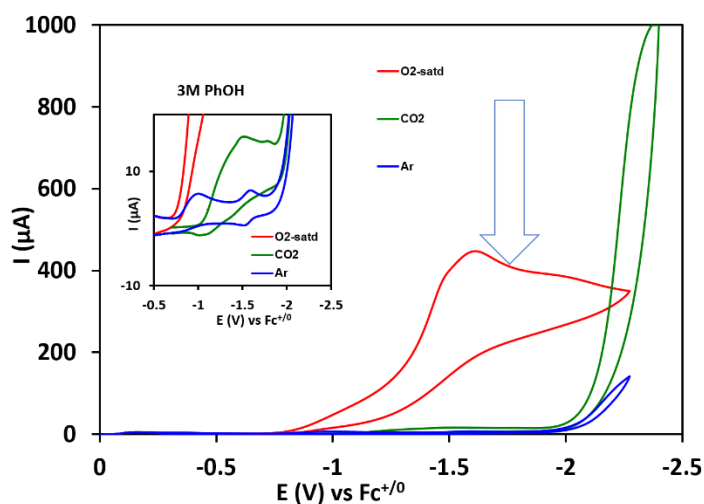


Figure S2. The CV of FeFc_4 with O_2 (red), in the presence of CO_2 (green) and in Ar (blue) in 3M PhOH in acetonitrile with edge plane pyrolytic graphite as working electrode, Pt counter and AgCl/Ag as reference electrode. 100 mM tetrabutylammonium perchlorate is used as supporting electrolyte. Scan rate = 100 mV/s. Inset: The CV region is zoomed in the inset. The dip of current at Fe(I/O) level is shown by a downward arrow.

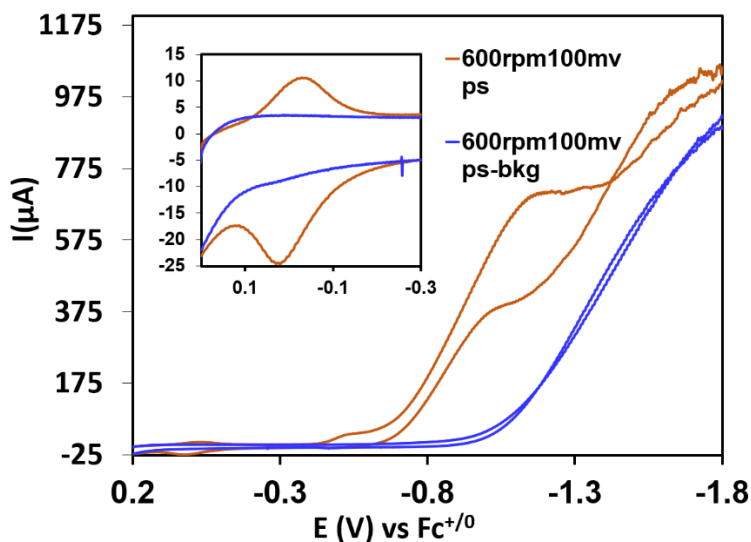


Figure S3. The CV of FeFc_4 in the presence of O_2 (orange) and without catalyst (blue) in 3M phenol in acetonitrile with edge plane pyrolytic graphite as working electrode, Pt counter and AgCl/Ag as reference electrode. 100 mM tetrabutylammonium perchlorate is used as supporting electrolyte. Scan rate = 100 mV/s. Rotation speed = 600 rpm. Inset: The CV region is zoomed in the inset.

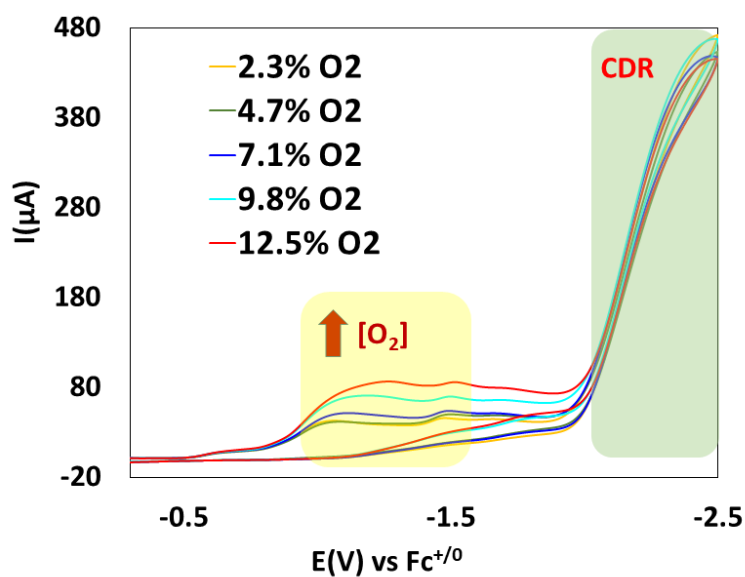


Figure S4. The CV of FeFc_4 in the presence of increasing oxygen and CO_2 , in 3M phenol in acetonitrile with glassy carbon as working electrode, Pt counter and AgCl/Ag as reference electrode. 100 mM tetrabutylammonium perchlorate is used as supporting electrolyte. Scan rate = 100 mV/s.

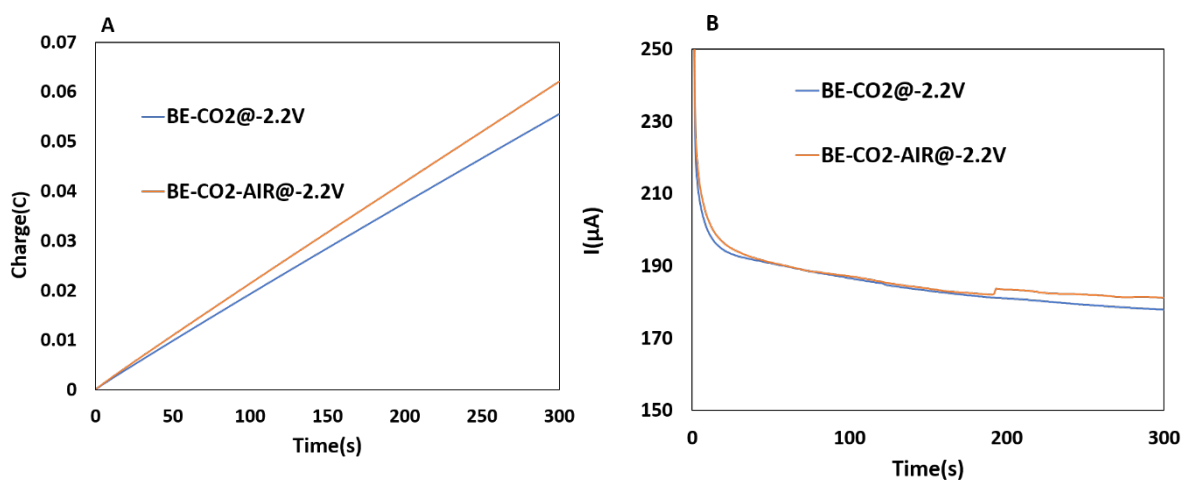


Figure S5. (A) Charge vs time plot for the constant potential electrolysis of FeFc_4 in the presence of CO_2 (blue) and CO_2 -oxygen (orange) (B) Current vs time plot for the constant potential electrolysis of FeFc_4 in the presence of CO_2 (blue) and CO_2 -oxygen (orange) at -2.2 V vs $\text{Fc}^{+/0}$ in 3M phenol in acetonitrile with glassy carbon as working electrode, Pt counter and AgCl/Ag as reference electrode. 100 mM tetrabutylammonium perchlorate is used as supporting electrolyte.

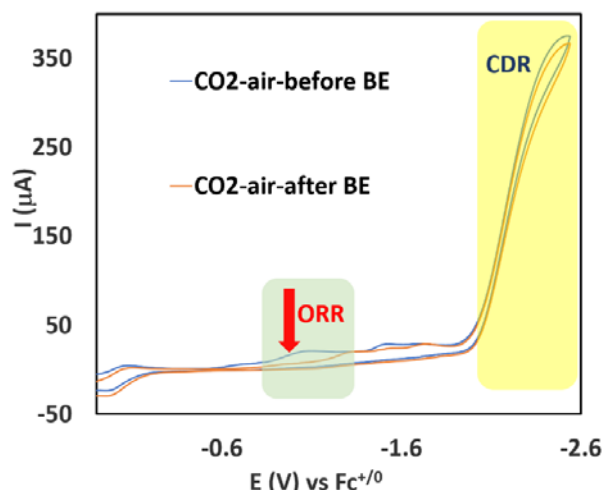


Figure S6. The CV of FeFc₄ before (cyan) and after (orange) bulk electrolysis at -2.2 V vs Fc^{+/0} in 3M phenol in acetonitrile with glassy carbon as working electrode, Pt counter and AgCl/Ag as reference electrode. 100 mM tetrabutylammonium perchlorate is used as supporting electrolyte. Scan rate = 100 mV/s.

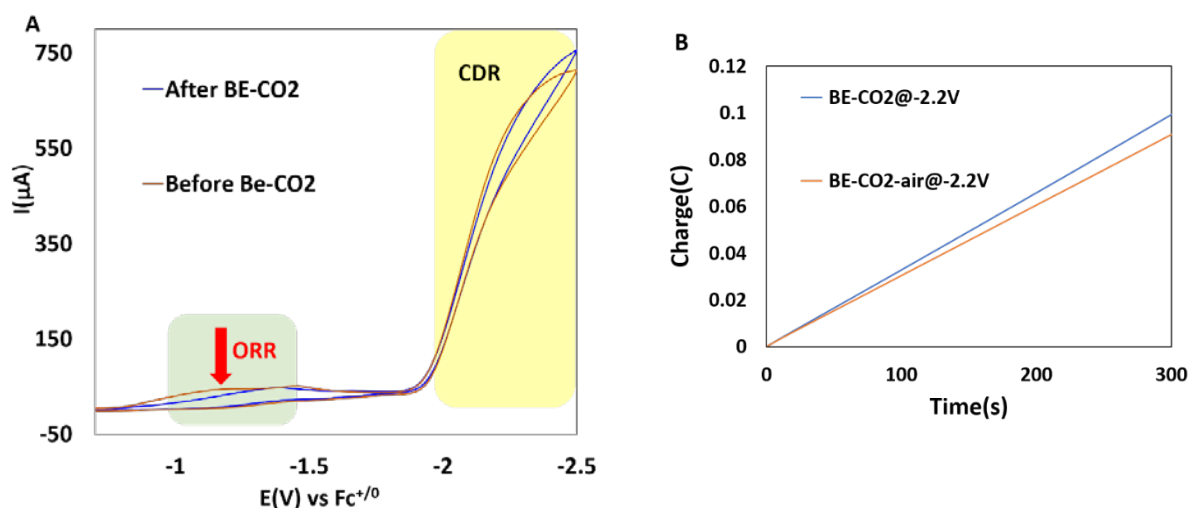


Figure S7. (A) The CV of FePf before (orange) and after (blue) bulk electrolysis at -2.2 V vs Fc^{+/0} in 3M phenol in acetonitrile with glassy carbon as working electrode, Pt counter and AgCl/Ag as reference electrode. 100 mM tetrabutylammonium perchlorate is used as supporting electrolyte. Scan rate = 100 mV/s. (B) Charge vs time plot for the constant potential electrolysis of FePf in the presence of CO₂ (blue) and CO₂-O₂ (orange) at -2.2 V vs Fc^{+/0} in 3M phenol in acetonitrile with glassy carbon as working electrode, Pt counter and AgCl/Ag as reference electrode. 100 mM tetrabutylammonium perchlorate is used as supporting electrolyte.

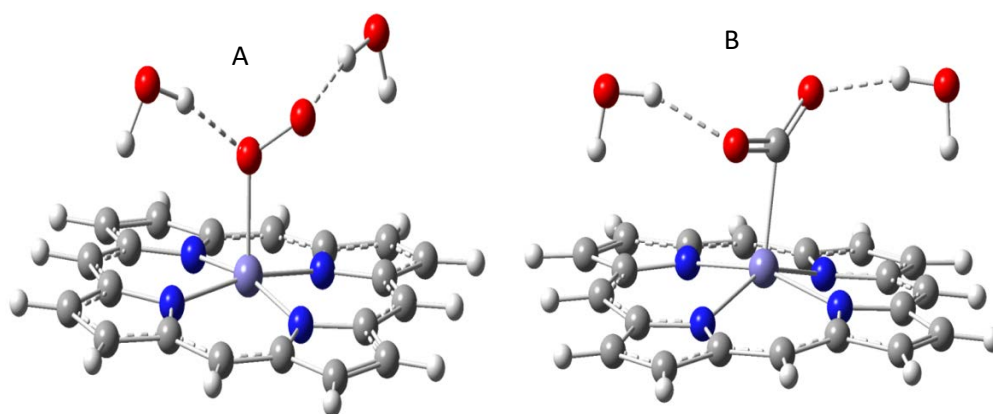


Figure S8. DFT optimized structures of (A) Fe(II)-O₂ adduct stabilized by H-bonding through water molecules (B) Fe(II)-CO₂²⁻ adduct stabilized by H-bonding through water molecules.

Table S1. Estimate of % PROS for various iron porphyrins of interest.

Complex	% PROS
FeTPP	26
Fe(tBu) ₄	47
FePf	25

Table S2. Estimate of % Faradaic yield for FeFc₄ during CO₂ reduction and ORR

FeFc ₄ %FY	in CO ₂	in O ₂
	92% CO, 0.5% formate	PROS: 6%, no catalyst decay, rest is H ₂ O

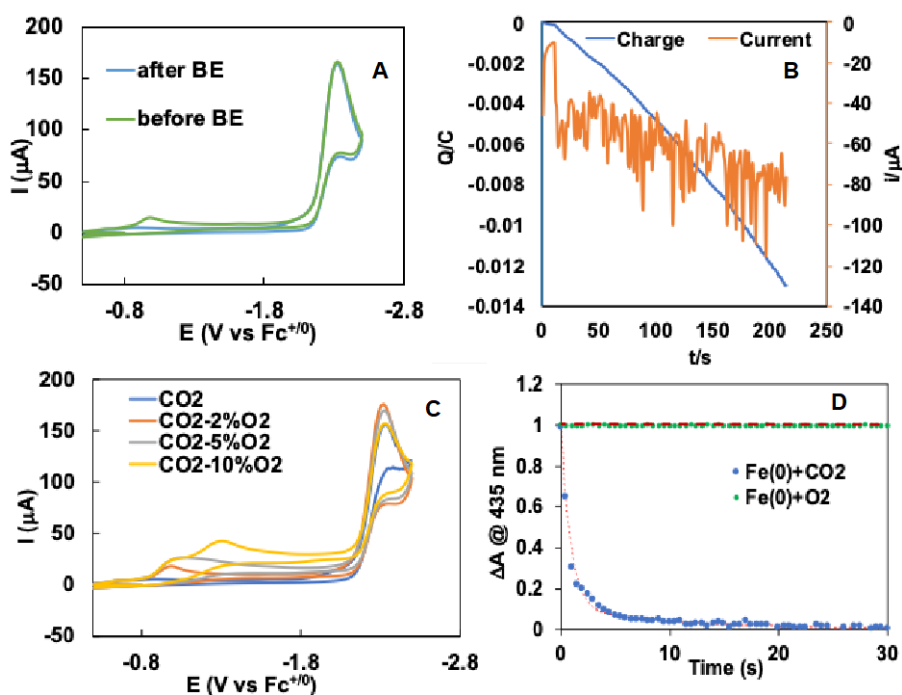


Figure S9. (A) The CV of FeTPP before (green) and after (blue) bulk electrolysis at $Fe(I/0)$ (B) Charge and Current vs time plot for the constant potential electrolysis of FeTPP (C) The CV of FeTPP in the presence of increasing oxygen and CO_2 ; electrolyte contains 100 mm tetrabutylammoniumperchlorate and 3M phenol (D) UV-Vis kinetic trace of the disappearance of the ~ 435 nm band as recorded in the reaction of $Fe(0)TPP$ with CO_2 (blue dots) and O_2 (green dots); the corresponding kinetic fit lines are also shown.

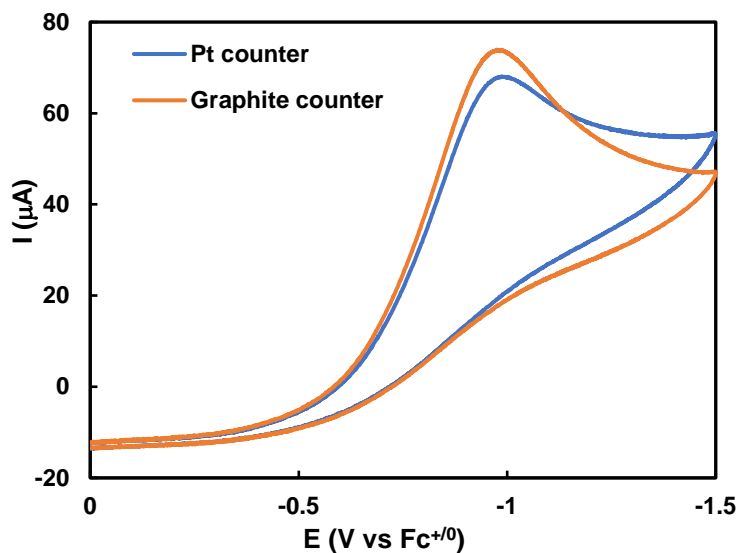


Figure S10. ORR with $FeFc_4$ using Pt as counter electrode (blue) and graphite as counter electrode (orange). Glassy carbon as working electrode and the electrolyte contains tetrabutylammonium perchlorate and phenol. Scan rate = 100 mV/s.

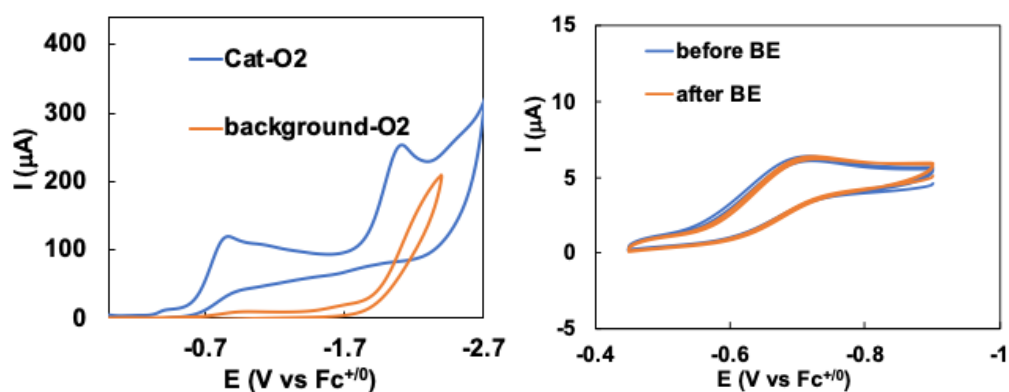


Figure S11. (left) CV of FeFc_4 in the presence of oxygen (blue) and in the absence of catalyst (orange); (right) CV of Fe(III/II) in Ar before (blue) and after (orange) electrolysis at Fe(I/0) level. Glassy carbon as working electrode and Pt as counter electrode are used. Electrolyte contains tetrabutylammoniumperchlorate and phenol. Scan rate = 100 mV/s.

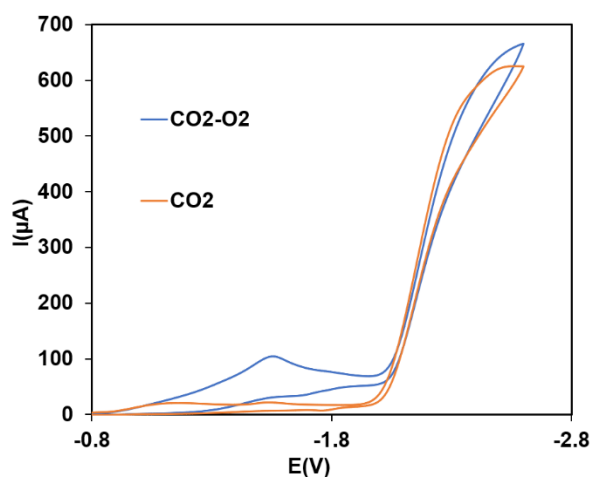


Figure S12. The CV of Fe(tBu)_4^7 in the presence of CO_2 (orange) and $\text{O}_2\text{-CO}_2$ mixture (blue); electrolyte contains 100 mM tetrabutylammoniumperchlorate and 3M phenol; Glassy carbon as working electrode and Pt as counter electrode; Scan rate = 100 mV/s.

Table S3. Optimized coordinates of Fe-CO₂ adduct stabilized by two water molecules (Fig. S8 B)XYZ

Fe	-0.39194916	-0.57203389	0.00000000
N	-2.16210916	0.09075111	-0.87368800
N	0.62793484	0.07586411	-1.74247200
N	1.42239884	-0.68936389	0.98625500
N	-1.29819016	-0.23426689	1.89720100
C	-2.65970916	-0.03762389	2.13038800
C	-2.93150416	-0.11962089	3.54150500
H	-3.91738516	0.00933311	4.00006700
C	-1.72708516	-0.39868689	4.16700400
H	-1.53865616	-0.55266289	5.23400500
C	-0.72452816	-0.48565989	3.12697300
C	0.64360384	-0.79415389	3.33762800
C	1.64633884	-0.84349089	2.34422300
C	3.06736484	-0.98937489	2.59762100
H	3.51355984	-1.13468089	3.58647100
C	3.70817184	-0.88946589	1.37668800
H	4.78328784	-0.92254489	1.17235700
C	2.68705284	-0.67285589	0.37990000
C	2.93498684	-0.37174889	-0.96642600
C	1.99922384	-0.01791389	-1.95624400
C	2.30004784	0.26237611	-3.33696000
H	3.30338384	0.26340611	-3.77568300
C	1.08927484	0.50098011	-3.96986700
H	0.91139584	0.72526911	-5.02642200
C	0.05740184	0.36034311	-2.96356300
C	-1.33863116	0.46625011	-3.19149800
C	-2.35734216	0.38400311	-2.21347500
C	-3.75737816	0.68326011	-2.45413000
H	-4.18160416	0.93988311	-3.43000900
C	-4.40351316	0.60659511	-1.23448700
H	-5.45911116	0.79635911	-1.01462800
C	-3.40527016	0.25875511	-0.25261400
C	-3.62032716	0.18790211	1.12988900
H	0.97109184	-0.90564189	4.37986100

H	3.98800384	-0.39869489	-1.28068600
H	-1.65455816	0.73486811	-4.20833600
H	-4.65501016	0.33133611	1.47139700
C	-0.83450316	-2.47655689	0.05850500
O	-0.40183816	-2.56611289	-1.12383900
O	-1.33909916	-3.21863189	0.90509000
O	-0.11542316	-3.98549989	3.41078600
H	0.25021284	-3.07812889	3.52239700
H	-0.60446216	-3.85310789	2.56174100
O	-1.71469616	-2.80540689	-3.67820700
H	-1.70444216	-1.82104389	-3.68384200
H	-1.30279316	-2.95932689	-2.79319700

Optimized coordinates of Fe-O₂ adduct stabilized by two water molecules (Fig. S8 A)

XYZ

Fe	-0.33812949	0.20863309	0.00000000
N	-2.12043049	0.68407609	-0.81751500
N	0.53285351	0.53551509	-1.79303600
N	1.47343751	0.15507509	0.84754500
N	-1.18268049	0.22951409	1.81220800
C	-2.52943249	0.38203709	2.12978600
C	-2.75000649	0.19589909	3.53828500
H	-3.72700049	0.26135209	4.02678900
C	-1.51283349	-0.08780891	4.10413600
H	-1.26662649	-0.28224091	5.15225400
C	-0.55938049	-0.05533891	3.03589300
C	0.82071251	-0.21947191	3.20310800
C	1.76357451	-0.09743591	2.19429600
C	3.18893251	-0.17175891	2.40786600
H	3.66068651	-0.34887291	3.37952700

C	3.78242351	0.03497109	1.18430000
H	4.84764451	0.04686709	0.93220700
C	2.71405651	0.21565509	0.22250000
C	2.92250451	0.39659909	-1.14364300
C	1.89380751	0.52942409	-2.09389100
C	2.10983751	0.68174109	-3.50590700
H	3.09385351	0.69888109	-3.98442400
C	0.85562751	0.77546009	-4.09693000
H	0.60407251	0.91385909	-5.15296300
C	-0.10312149	0.69874109	-3.03457100
C	-1.48757249	0.83774309	-3.20510300
C	-2.41716749	0.85843709	-2.17605900
C	-3.82776049	1.10122709	-2.36719500
H	-4.29917749	1.27652809	-3.33943200
C	-4.40468249	1.08147409	-1.11877700
H	-5.45569549	1.22248609	-0.84719600
C	-3.34551849	0.80838209	-0.16883700
C	-3.54630249	0.67576209	1.20284700
H	1.18410951	-0.43405891	4.21663000
H	3.95725051	0.40842309	-1.50807300
H	-1.85881149	0.97046009	-4.22981000
H	-4.56977549	0.77632209	1.58471200
O	-0.16703949	-2.41956491	0.68029400
H	-1.50346649	-2.96018991	1.78899600
O	0.25114551	-2.64299191	-2.91172200
H	0.46844351	-1.75545691	-3.26644200
H	-0.00612149	-2.40898091	-1.98535500
O	-2.14312949	-3.19764491	2.52191800

H	-2.24768649	-2.32243091	2.95230900
O	-0.52286249	-1.55962191	-0.29196100

References

1. Samanta, S.; Sengupta, K.; Mittra, K.; Bandyopadhyay, S.; Dey, A. Selective Four Electron Reduction of O₂ by an Iron Porphyrin Electrocatalyst Under Fast and Slow Electron Fluxes, *Chem. Commun.* **2012**, 48, 7631-7633.
2. Wuenschell, G. E.; Tetreau, C.; Lavalette, D.; Reed, C. A. Hydrogen-bonded Oxyhemoglobin Models with Substituted Picket-fence Porphyrins: The Model Compound equivalent of Site-directed Mutagenesis. *J. Am.Chem.Soc.* **1992**, 114, 3346-3355.
3. Costentin, C.; Passard, G.; Robert, M.; Savéant, J. M. Ultraefficient Homogeneous Catalyst for the CO₂ to CO Electrochemical Conversion. *Proc. Natl. Acad. Sci.* **2014**, 111, 14990-14994.
4. Mondal, B.; Rana, A.; Sen, P.; Dey, A. Intermediates Involved in the 2e⁻/2H⁺ Reduction of CO₂ to CO by Iron(0) Porphyrin, *J. Am. Chem. Soc.* **2015**, 137, 11214-11217.
5. Mashiko, T.; Reed, C. A.; Haller, K. J.; W. R. Scheidt, Nature of Iron(I) and Iron(0) tetraphenylporphyrin Complexes. Synthesis and Molecular Structure of (dibenzo-18-crown-6)bis(tetrahydrofuran)sodium(meso-tetraphenylporphinato)ferrate and bis[tris(tetrahydrofuran)sodium] (meso-tetraphenylporphinato)ferrate *Inorg. Chem.* **1984**, 23, 3192-3196.
6. Frisch, M. J.; Trucks, G. W.; Schlegel, H. B.; Scuseria, G. E.; Robb, M. A.; Cheeseman, J. R.; Scalmani, G.; Barone, V.; Mennucci, B.; Petersson, G. A.; Nakatsuji, H.; Caricato, M.; Li, X.; Hratenian, H. P.; Izmaylov, A. F.; Bloino, J.; Zheng, G.; Sonnenberg, J. L.; Hada, M.; Ehara, M.; Toyota, K.; Fukuda, R.; Hasegawa, J.; Ishida, M.; Nakajima, T.; Honda, Y.; Kitao, O.; Nakai, H.; Vreven, T.; Montgomery Jr., J. A.; Peralta, J. E.; Ogliaro, F.; Bearpark, M.; Heyd, J. J.; Brothers, E.; Kudin, K. N.; Staroverov, V. N.; Kobayashi, R.; Normand, J.; Raghavachari, K.; Rendell, A.; Burant, J. C.; Iyengar, S. S.; Tomasi, J.; Cossi, M.; Rega, N.; Millam, J. M.; Klene, M.; Knox, J. E.; Cross, J. B.; Bakken, V.; Adamo, C.; Jaramillo, J.; Gomperts, R.; Stratmann, R. E.; Yazyev, O.; Austin, A. J.; Cammi, R.; Pomelli, C.; Ochterski, J. W.; Martin, R. L.; Morokuma, K.; Zakrzewski, V. G.; Voth, G. A.; Salvador, P.; Dannenberg, J. J.; Dapprich, S.; Daniels, A. D.; Farkas, Ö.; Foresman, J. B.; Ortiz, J. V.; Cioslowski, J.; Fox, D. J.; C.02 ed, *Gaussian*, Inc., Wallingford, CT, **2004**.
7. Sen, P.; Mondal, B.; Saha, D.; Rana, A.; Dey, A. Role of 2nd Sphere H-bonding Residues in Tuning the Kinetics of CO₂ Reduction to CO by Iron Porphyrin Complexes. *Dal. Trans.* **2019**, DOI: 10.1039/C8DT03850C

